ISSN 1392–1320 MATERIALS SCIENCE (MEDŽIAGOTYRA). Vol. 12, No. 4. 2006

# Formation of Metaloorganic Multilayer Structures by Langmuir-Blodgett Technique

**Irina ČERNIUKĖ[1*], Sigitas TAMULEVIČIUS[1,2], Igoris PROSYČEVAS[2], Judita PUIŠO[1,2], Asta GUOBIENĖ[2], Mindaugas ANDRULEVIČIUS[2]**

[1]*Department of Physics, Kaunas University of Technology, Studentų 50, LT-51368 Kaunas, Lithuania*
[2]*Institute of Physical Electronics, Kaunas University of Technology, Savanorių 271, LT-50131 Kaunas, Lithuania*

*Received 25 May 2006; accepted 20 October 2006*

The preliminary results on the formation of Langmuir-Blodgett (LB) multilayers and following sulphidization are presented. Well-known techniques to visualise the morphology, assess optical characteristics, thickness and chemical composition of mono- and multilayers on different substrates (atomic force microscopy, ellipsometry and X-ray photoelectron spectroscopy) were used to analyze produced multilayer structures. It is shown that roughness of the produced metallorganic layers containing Ni and Cu depends on the roughness of the substrate (Si, PET, $SiO_2$), number of layers as well as on the following sulphidization procedure.
*Keywords*: Langmuir-Blodgett technique, Langmuir-Blodgett mono- and multilayer, AFM, XPS, ellipsometry.

## 1. INTRODUCTION

The microelectronics and optical industries require the manufacture of complex thin-film structures with precise order, composition, and thickness [1 – 4]. The oldest method for manufacturing thin organized monolayers is the Langmuir-Blodgett (LB) technique. An insoluble monolayer of typically a long chain fatty acid or phospholipid is spread on water and with care and luck can be transferred to a solid substrate (Fig. 1).

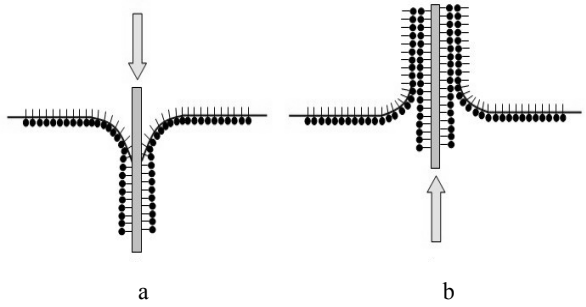


**Fig. 1.** Schematic illustration of LB deposition (Y type LB layers). Sticks represent the hydrophobic ends of the molecules and circles represent the hydrophilic ends of the molecules. The grey rectangle represents the substrate. (a) As the substrate passes through the surface, hydrophobic ends stick to the hydrophobic substrate (e.g., glass slide). (b) As the substrate is withdrawn hydrophilic ends stick to the hydrophilic ends of the deposited film [1]

Depending on the material, substrate and deposition speed, LB multilayers can have various structures and can be classified into three basic categories: X, Y and Z type (Fig. 2). Applications of LB films have proved to be elusive, due to their fragility but we can use them principally as model systems, for example, in the fabrication of biomembranes (Fig. 2, Y type), and for studying templating of materials. However, if we sulphidate or oxidize obtained LB layers, we can get more applicable thin films, that can be useful components in many practical and commercial applications such as sensors, detectors, displays and electronic circuit components [5 – 7]. High thickness resolution and low cost of the technology allow considering it as very perspective method for the applications, where ultrathin semiconductor layers must be used, such as electronics and optoelectronics [3].

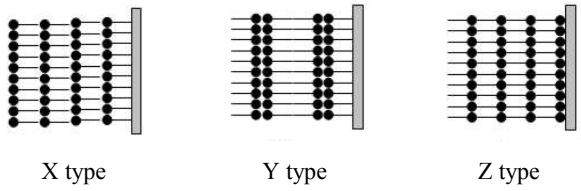


**Fig. 2.** Three basic categories of LB structures: X, Y and Z type [1]

The prevalence of using the LB technique is due to its advantages: a) ability to produce a very consistent thickness; b) smoothness of LB films, c) ability to coat surfaces without harming the surface; d) LB films are capable of assembling molecules into a well-defined, stable structure; e) individual monolayers could be created with high consistency of thickness, it could be adjusted by changing the distance between the molecules; f) cheap technology, that does not require high vacuum or temperatures. Of course, the LB technique also has some disadvantages: a) LB films have limited resistivity to high temperatures; b) substrate should be very smooth; c) substrate must be dipped into the aquae's solution; d) slow deposition; e) not all materials are suitable for LB deposition.

Many studies have been carried out on synthesis and analysis of NiS and CuS LB films [3, 7 – 10]. Authors used different acids and complexes as carriers, and different methods to sulphidate LB layers. In [11 – 12] works other different ways of NiS and CuS synthesis and their application in gas sensors are presented.

*Corresponding author. Tel.: +370-37-351028; fax: +370-37-456475. E-mail address: *IriBurl@merkys.ktu.lt* (I. Černiukė)

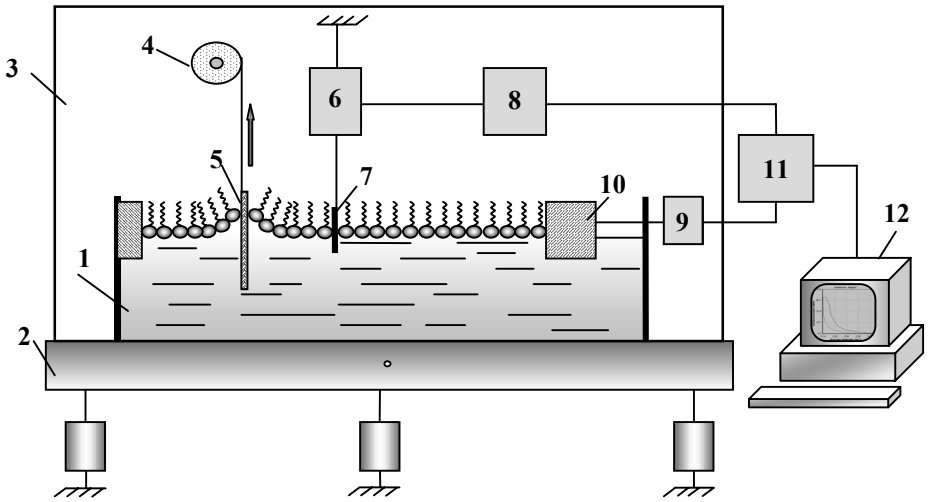


**Fig. 3.** Schematic diagram of the Langmuir-Blodgett equipment. 1 – trough, 2 – vibration-proof table, 3 – transparent hermetic block, 4 – substrate pulling and dipping mechanism, 5 – substrate, 6 – surface pressure sensor, 7 – Wilhelmi plate, 8, 9 – motors, 10 – horizontal barrier, 11 – control electronic unit, 12 – personal computer [1]

The main idea of this research was to create LB ordered, mono- and multilayred nickel and/or copper contained thin films on Si, PET and $SiO_2$ substrates, and then to sulphidate them. As carriers we used behenic and stearic acids. Sulphidize of the LB film of the complexes was carried out by reacting with $Na_2S$ (dissolved in isopropyl alcohol) [7].

## 2. EXPERIMENTAL

During LB deposition thin films are deposited layer by layer by passing the substrate through a floating monolayer. In our experiment we have used the Langmuir-Blodgett equipment, schematic diagram of which is like in [1] and it is shown in Fig. 3. LB equipment includes five main components: LB through, barrier, surface pressure sensor – Wilhelmi plate (accuracy ~0.1 mN/m), control electronic unit and software package for the device control and data acquisition (for PC).

In this work we used solutions of behenic ($CH_3(CH_2)_{20}COOH$) and stearic ($CH_3(CH_2)_{16}COOH$) acids, and nickel sulphate ($NiSO_4$) and copper sulphate ($CuSO_4$). Behenic and stearic acids were solved in chloroform by ratio 1 mg/1ml. Obtained solutions were kept at least for 15 min at 30 °C – 40 °C temperature. After that they were spread on $10^{-3}$ M $NiSO_4$ and $CuSO_4$ subphases, respectively. In preparing $NiSO_4$ and $CuSO_4$ solutions we used distilled water (18.2 MΩ cm resistivity).

Isotherms were taken at a compression rate of 0.7 mm/s, and the temperature of the aqueous subphase was maintained at 20.0 ±0.1 °C. Monolayers were spread on pure water or on aqueous metal halides and incubated for 30 min before starting the compression.

The monolayer transfer onto the substrates was carried out by the vertical mode at surface pressure of 30 mN/m and deposition rate of 0.05 mm/s. Pause between the steps (drying time) was 2 min. The employed substrates were: n-type silicon (Si) with orientation <111> and thickness 318 μm; polyethylene terephthalate (PET), thickness 100 μm; quartz glass ($SiO_2$), thickness 500 μm. Before the deposition the substrates were cleaned in $O_2$ plasma (Si, $SiO_2$ – 2 min, PET – 1 min).

To sulphidize the obtained LB layers we put them into $Na_2S$ solved in isopropyl alcohol solution for 20 minutes.

Ellipsometrical parameters $\psi$ and $\Delta$ parameters, refractive index and thickness to obtained LB layers were measured by a laser ellipsometer Gaertner L-115 ($\lambda$ = = 632.8 nm). Surface morphology and roughness of the LB layers were analyzed and assessed by an atomic force microscope (AFM) Nanotop NT-206 using contact-static scanning mode (cantilever force constant equal to 1.2 N/m).

Surface of the Ni containing film was analyzed with the X-ray Photoelectron Spectroscopy (XPS) method. The "Kratos Analytical XSAM800" spectrometer with non-monochromatized Al K$\alpha$ radiation ($h\nu$ = 1486.6 eV) was used. Energy scale of the system was calibrated according to Au 4f7/2 and Cu 2p3/2 Ag 3d5/2 peaks position. The C 1s, Ni 2p, S 2p, and O 1s spectra were determined at the 20 eV pass energy (0.1 eV energy increment) and the analyzer being in the fixed analyzer transmission (FAT) mode. Carbon, oxygen, sulphur, and nickel relative atomic concentration were calculated from the appropriate peak area with respect to sensitivity factors, using original KRATOS software. The "XPSPEAK41" software was employed to perform peak fitting procedure. The "MakroBeam" ion gun with 3.0 KeV energy of $Ar^+$ ions and current density 18 μA/cm$^2$ was used for Ni containing films surface sputtering. Sputtering time for Ni behenate and $NiS_x$ films were 30 s.

## 3. RESULTS AND DISCUSSIONS

### 3.1. Kinetics of the deposition

Fig. 4 shows surface pressure $\pi$ vs area $A$ isotherm curves of the stearic acid on $Ni^{2+}$ ion containing aqueous subphase when the compression speed of the barrier is 0.7 mm/s. We get two isotherm curves, one – when the barrier moved forwards, another – when the barrier moved backwards. For the isotherm (forwards) we found rapid increase of the surface pressure passing 0.21 nm$^2$ of molecular area. From this $\pi - A$ isotherm curve, we found the molecular area of stearic acid on $NiSO_4$ subphase is

**Table 1.** Ellipsometrical parameters $\psi$ and $\Delta$, refractive index and thickness of the LB layers

| Sample | *psi* | *delta* | *n* | $d_0$, nm | $d_{theor}$, nm | $E_d$, % |
|---|---|---|---|---|---|---|
| NiBeh/Si (5z) | 32 | 159 | 1.5 | 36 | 30 | 17 |
| NiBeh/Si (30y) | 33 | 206 | 1.6 | 176 | 155 | 14 |
| CuSt/Si (5y) | 31.5 | 177 | 1.6 | 28 | 30 | 6.7 |
| NiBehCuSt/Si (10y) | 34 | 142 | 1.6 | 63 | 55 | 15 |
| CuS/Si (5y) | 32 | 167 | 1.5 | 31 | 30 | 3.3 |
| NiSCuS/Si (10y) | 33 | 150 | 1.5 | 54 | 55 | 1.8 |
| HBeh/Si (5z) | 31.5 | 161 | 1.6 | 30 | 30 | 0 |
| NiBeh/Si (1z) | 31.5 | 174 | 1.5 | 15 | 15 | 0 |

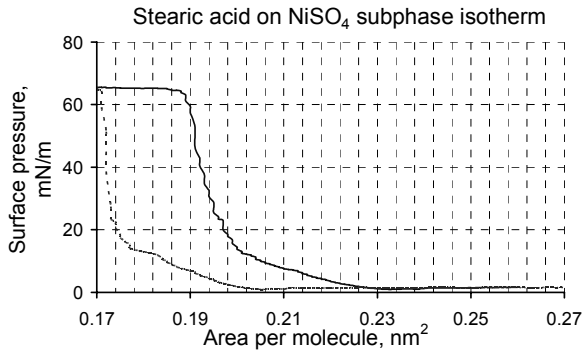


**Fig. 4.** Surface pressure – area isotherms of stearic acid on $Ni^{2+}$ containing $NiSO_4$ subphase. Barrier moved forwards (solid line), barrier moved backwards (dashed line)

0.20 $nm^2$ by extrapolating from the steepest curve regions to zero $\pi$ after rounding of to two decimal places. The surface pressure of the collapse ($\pi_{col}$) is about 65.2 mN/m. Backwards isotherm curve shows, that the compressing process is not recursive, because once the monolayer reaches collapse, it will never come to the initial gas state phase in the same amount. This shows reduced area per molecule.

Table 1 gives ellipsometrical parameters, refractive index and thickness of our LB layers on Si substrates. We consider that the height of layer one molecular (behenate and stearate) is about 2.5 nm, and multiplying this number by number of layers and by 2 (because we get monolayer when we dip and also when we pull out the substrate, also we have to add the thickness of hidrofobisation by depositing 1Z monolayer), we get the theoretical thickness $d_{theor}$ of the obtained LB layers. One can see, the relative thickness errors $E_d$ errors do not outmeasure 17 %. During this experiment the maximum number of layers that we deposited is 30 Y bilayers of nickel behenate on Si substrate. Thickness of this structure is 176 nm. Produce of gas sensors needs for layers of thickness about 100 nm. The minimum controlled thickness were able to produce was 15 nm.

## 3.2. ROUGHNESS OF THE LAYERS

AFM images and roughness of the obtained LB layers on Si, PET and $SiO_2$ substrates are shown in Fig. 5. The first row in Fig. 5 represents the morphology of clean substrates. PET is an optical polymer that has three-dimensional surface structure, and it is very rough as compared to the polished crystalline silicon or quartz. $SiO_2$ is amorphous and very smooth ($R_q$ is only 0.03 nm) [13]. Comparing AFM images of the samples with LB layers with the images of the clean substrates, we can see how the roughness of the substrates varies with the number of layers, type and chemical composition of the layer. Almost in all cases increasing the number of layers, results increase of roughness increasing too. It is interesting to note, that the maximum roughness for the deposited layers remains is the LB layers on PET substrates. This can mean that LB layers cover well the substrate repeating features of the surface morphology surface.

AFM images and roughness of LB layers on Si substrate after sulphidisation are shown in Fig. 6. As we can see, in the case of multilayers, sulphidizsation brings to the decrease of roughness (from 8.9 nm to 1.2 nm). Comparing LB layers before sulphidisation and after, we can see, that NiS (1Z) roughness increased from 0.4 nm to 8.9 nm, NiS (5Z) roughness increased from 5.5 nm to 7.3 nm, CuS(5Y) roughness increased from 0.3 nm to 3.4 nm, and NiSCuS (10Y) roughness decreased from 1.5 nm to 1.2 nm. In conclusion, we can say, that after sulphidization of homogeneous LB layers, the roughness increases, and after sulphidization of heterogeneous LB layers, the roughness decreases. The initial LB monolayer influences the morphology of posterior monolayers.

## 3.3. CHEMICAL COMPOSITION OF THE LB LAYERS

After primary measurements, surface of the samples were sputtered with $Ar^+$ ions for 30 s. In Table 2 surface atomic concentration of LB layers on Si substrate before and after sputtering is given.

**Table 2.** Surface atomic concentration of LB layers on Si substrate (before and after suputtering)

| | Ni, % | O, % | C, % | Si, % | S, % |
|---|---|---|---|---|---|
| NiBeh(30Y) | 0.27 | 18.11 | 80.28 | 1.33 | – |
| NiBeh(30Y) after sputter. | 0.45 | 8.52 | 89.46 | 1.57 | – |
| NiS (5Z) | 0.37 | 15.29 | 79.61 | 1.30 | 3.43 |
| NiS(5Z) after sputter. | 0.62 | 18.74 | 71.75 | 6.21 | 2.67 |

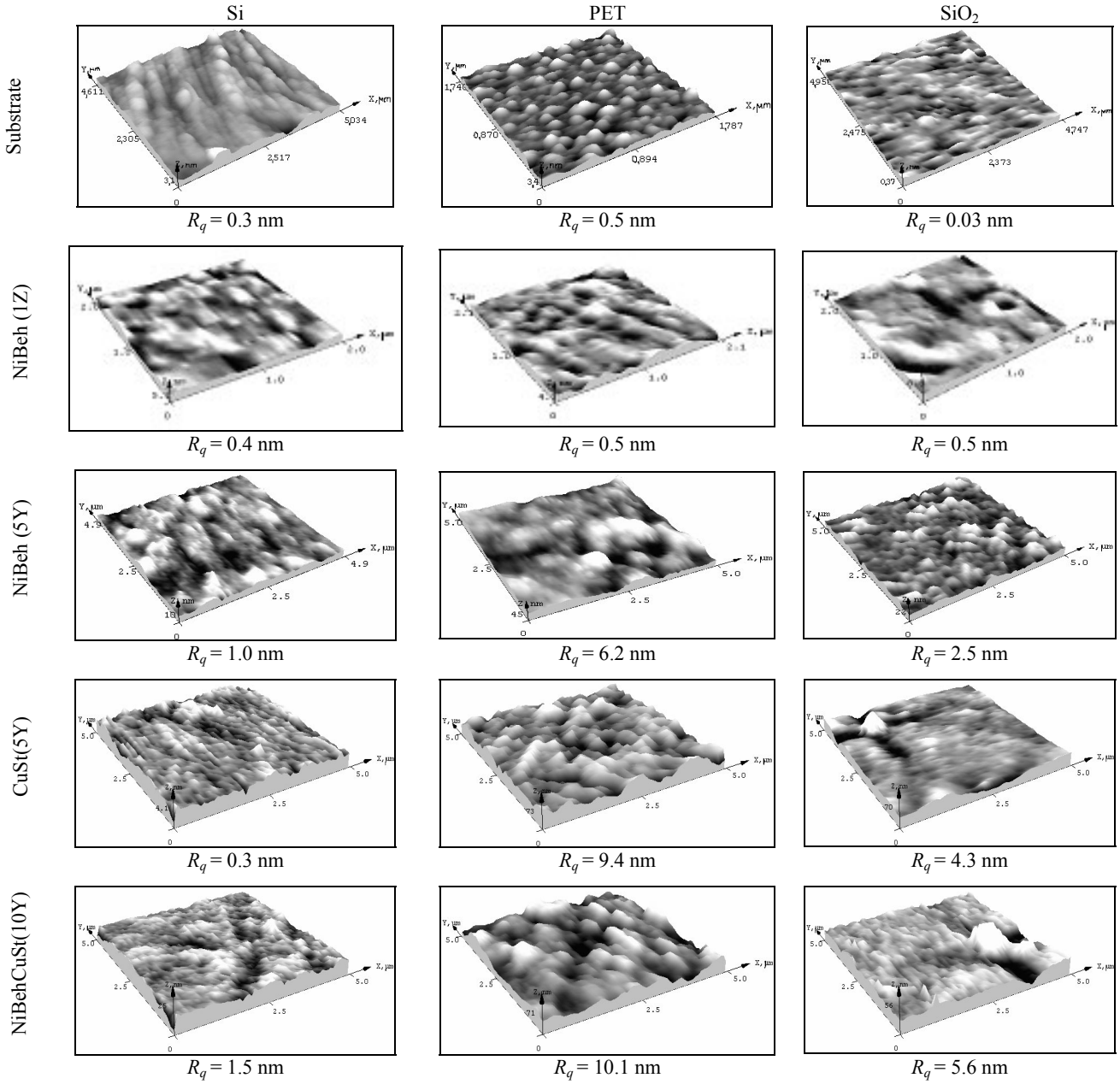


**Fig. 5.** AFM images and corresponding roughness ($R_q$) of different LB layers on Si, PET and $SiO_2$ substrates

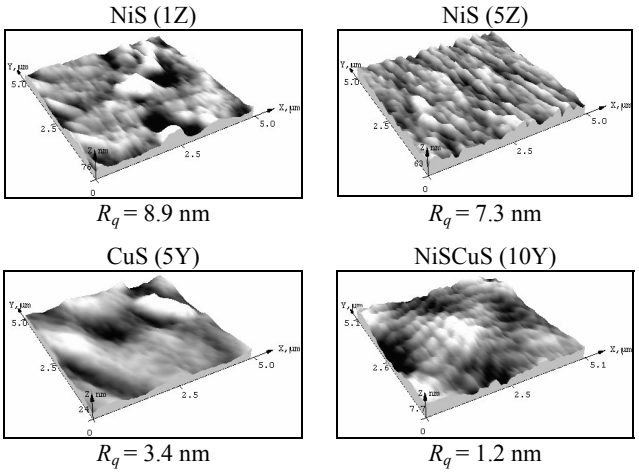


**Fig. 6.** AFM images and roughness ($R_q$) of different LB layers on Si substrate after sulphidisation

**Table 3.** Chemical composition of NiBeh (30Y) on Si substrate after suputtering

| | Experimental values | | | Theoretical [12] | |
|---|---|---|---|---|---|
| peak | $E_b$, eV | Chem. Bind. | Area, % | $E_b$, eV | Chem. compound |
| 1 | 852.70 | Ni_metal | 23 | 852.8 | Ni |
| 2 | 854.43 | Ni-C-O-H | 64 | 854.5 | $[Ni(C_6H_5C(O)CHC(O)C_6H_5)_2]$ |
| 3 | 856.40 | Ni-S-O | 13 | 856.9 | $NiSO_4$ |

As we see, after surface sputtering by $Ar^+$ ions, the adsorbed contaminant is removed, but also with it, we removed the superficial LB layers. This shows increased Ni and Si concentration in both samples, and decreased sulphur concentration in NiS(5Z). In our obtained samples, we get Ni 0.45 % and 0.62 % of total surface atomic concentration, in NiBeh and NiS, respectively.

Tables 3 and 4, and Fig. 7 give us chemical composition after sputtering of NiBeh (30Y) and NiS (5Z) on Si substrate. XPS spectra of Ni 2p of sputtered LB layers of NiBeh (30Y) on Si substrate and NiS (5Z) on Si substrate after peak fitting procedure with "XPSPEAK41" software [11] are shown in Fig. 7. Comparing the experimental values of obtained binding energies with the theoretical ones [11], we can determine possible chemical bindings of Ni. According to this analysis we determine $NiS_x$ chemical binding in NiS (5Z) sample.

**Table 4.** Chemical composition of NiS (5Z) on Si substrate after sputtering

| | Experimental values | | | Theoretical values [12] | |
|---|---|---|---|---|---|
| peak | $E_b$, eV | Chem. Bind. | Area, % | $E_b$, eV | Chem. compound |
| 1 | 852.8 | Ni_metal | 16.5 | 852.7 | Ni |
| 2 | 853.6 | $NiS_x$ | 46.5 | 853.0 | NiS |
| 3 | 854.6 | Ni-C-S-H | 37.0 | 854.7 | [Ni(-C--6H5S)$_2$] |

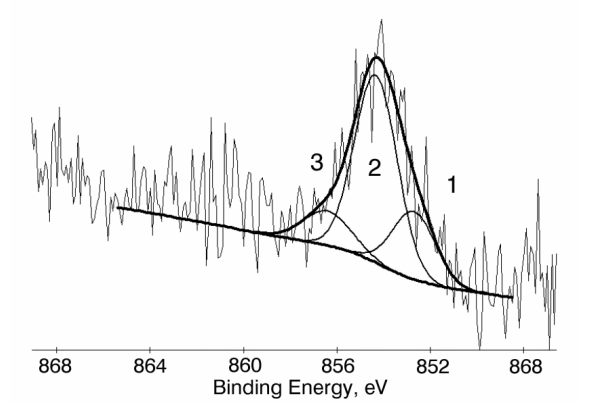


a

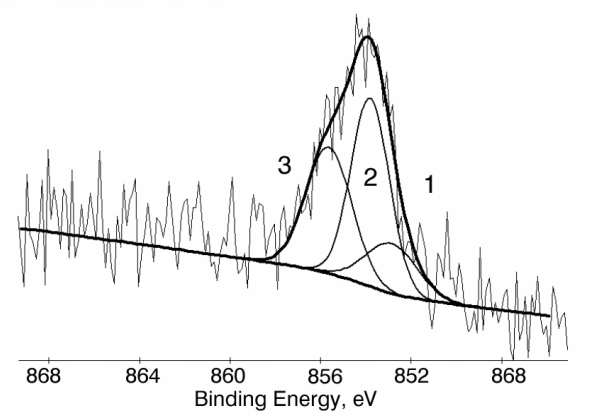


b

**Fig. 7.** XPS spectra of Ni2p of sputtered LB layers of (a) NiBeh (30Y) on Si substrate, (b) NiS (5Z) on Si substrate. (Notifications of the peaks 1, 2, 3, are given in Table 3 and Table 4)

## CONCLUSION

LB layers roughness is dependent on the substrate, LB deposition type and subphase solution. It is varied from 0.4 nm to 5.6 nm. After sulphidazation the roughness of the LB layers decrease seven times. The thickness of the LB layers varied from 15 nm to 176 nm and refractive index was 1.6.

XPS analysis shows that LB method allows formation metal organics ultra thin films. 0.45 % of Ni in nickel behenate (30Y) sample and 0.62 % of Ni in the nickel sulphide (5Z) sample was found. From the XPS spectra we have identified $NiS_x$ chemical binding in NiS (5Z) sample, that means that we can control not only the thickness and roughness of the LB layers, but their chemical composition as well.

## *Acknowledgement*

This work is partially supported by the Lithuanian State Science and Studies Foundation. Thanks to Vitoldas Kopustinskas for ellipsometry measurements.

**REFERENCES**

1. **Roberts, G.** Langmuir-Blodgett Films. Plenum Press, New York and London, 1990.
2. **Werkman, P. J.** Langmuir-Blodgett Film Formation of Polymerisable Amphiphilic Metal Complexes (A structural investigation). *Ph.D. Thesis*, 1998, ISBN 90-367-0799-4.
3. **Erokhina, S., Erokhin, V., Nicolini, C.** Electrical Properties of Thin Copper Sulfide Films Produced by the Aggregation of Nanoparticles Formed in LB Precursor, *Colloids and Surfaces A*: *Physicochem. Eng. Aspects* 198 – 200 2002: pp. 645 – 650.
4. **Smotkin, E. S., Lee, C., Bard, A. J., Campion, A., Fox, M. A., Mallouk, T. E., Webb, S. I., White, J. M.** Size Quantization Effects in Cadmium Sulfide Layers Formed by a Langmuir-Blodgett Technique *Chem. Phys. Lett.* 152 1988: p. 265.
5. **Erokhin, V., Troitsky, V., Erokhina, S., Mascetti, G., Nicolini, C.** In Plane Pattering of Aggregated Nanoparticle Layers *Langmuir* 18 2002: pp. 3185 – 3190.
6. **Hemakanthi, G., Dhathathreyan, A., Ramasami, T.** Organization of Copper Nanoclusters in Langmuir-Blodgett Films *Bull. Mater. Sci.* 1 (25) 2002: pp. 1 – 5.
7. **Hemakanthi, G., Dhathathreyan, A.** Synthesis of Nickel Sulphide Using Langmuir-Blodgett Films of Nickel Complex of 2-hydroxy-5-nitro-N-benzylidene Hexadecylamine Monolayers at Air/Water Interface *Chem. Phys. Lett.* 334 2001: pp. 245 – 249.
8. **Vidya, V., Ambily, S., Narang, S. N., Major, S., Talwar, S. S.** Development of Metal Sulfide-poly (3-octylthiophene) Composite LB Multilayers *Colloids and Surfaces A*: *Physicochem. Eng. Aspects* 198 – 200 2002: pp. 383 – 388.
9. **Werkman, P. J., Wieringa, R. H., Schouten, A. J.** The Formation of Copper Sulphide Semiconductors Inside Langmuir–Blodgett Films of Cu(II) Ion Complexes *Thin Solid Films* 323 1998: pp. 251 – 256.
10. **Hemakanthi, G., Dhathathreyan, A., Ramasami, T., Mobius, D.** Formation of Nickelhydroxy Sulfide Precursor and Nickel Sulfide in Langmuir and Langmuir-Blodgett Films of a Nickel Complex of Octadecylsuccinic Acid *Thin Solid Films* 384 2001: pp. 206 – 211.
11. http://www.phy.cuhk.edu.hk/~surface (April, 2005).
12. **Wagner, C. D., Naumkin, A. V., Anna Kraut-Vass A., Allison J. W Cedric, Powell J. Rumble Jr. J.R.** NIST Standard Reference Database 20, Version 3.4
13. **Tamulevičius, S., Prosyčevas, I., Guobienė, A., Puišo, J.** Oxygen Plasma Processing of Silicon and Silica Substrates for Thin Films of Polymer Blends *Solid State Phenomena ISSN 1012-0394* Trans Tech Publications Ltd, Uetikon-Zurich Switzerland ISSN 0040-6090 Vol. 99 – 100, 2004: pp. 175 – 178.

*Presented at the National Conference "Materials Engineering'2006" (Kaunas, Lithuania, November 17, 2006)*